Current Biology 17, 659–667, April 17, 2007 ©2007 Elsevier Ltd All rights reserved DOI 10.1016/j.cub.2007.02.044

Article

A Systems-Biology Analysis of Feedback Inhibition in the Sho1 Osmotic-Stress-Response Pathway

Nan Hao,[1] Marcelo Behar,[2] Stephen C. Parnell,[1] Matthew P. Torres,[1] Christoph H. Borchers,[1] Timothy C. Elston,[3] and Henrik G. Dohlman[1,3,*]
[1] Department of Biochemistry and Biophysics
[2] Department of Physics and Program in Molecular and Cellular Biophysics
[3] Department of Pharmacology
University of North Carolina at Chapel Hill
Chapel Hill, North Carolina 27599

Summary

Background: A common property of signal transduction systems is that they rapidly lose their ability to respond to a given stimulus. For instance in yeast, the mitogen-activated protein (MAP) kinase Hog1 is activated and inactivated within minutes, even when the osmotic-stress stimulus is sustained.
Results: Here, we used a combination of experimental and computational analyses to investigate the dynamic behavior of Hog1 activation in vivo. Computational modeling suggested that a negative-feedback loop operates early in the pathway and leads to rapid attenuation of Hog1 signaling. Experimental analysis revealed that the membrane-bound osmosensor Sho1 is phosphorylated by Hog1 and that phosphorylation occurs on Ser-166. Moreover, Sho1 exists in a homo-oligomeric complex, and phosphorylation by Hog1 promotes a transition from the oligomeric to monomeric state. A phosphorylation-site mutation ($Sho1^{S166E}$) diminishes the formation of Sho1-oligomers, dampens activation of the Hog1 kinase, and impairs growth in high-salt or sorbitol conditions.
Conclusions: These findings reveal a novel phosphorylation-dependent feedback loop leading to diminished cellular responses to an osmotic-stress stimulus.

Introduction

All living organisms can initiate distinct developmental programs depending on the presence of specific external cues. In many cases, those cues lead to activation of protein kinases, which in turn regulate a variety of cellular behaviors including metabolism, gene expression, cell division, cell motility, differentiation, and death [1]. Such cellular behaviors are commonly regulated by a single MAP kinase, but the response may depend on discrete changes in the intensity or duration of kinase activity. In one oft-cited example, epidermal growth factor promotes transient activation of the ERK MAP kinase and leads to cell proliferation, whereas nerve growth factor promotes sustained ERK activation and results in cell differentiation [2]. Moreover, abnormal or inappropriate activation of MAP kinase activity can lead to disorders such as asthma, autoimmune diseases, and cancer.

Despite the importance of temporal regulation in signal transduction, the underlying mechanisms leading to pathway inactivation are often poorly defined. Most work in this regard has focused on feedback inhibition through phosphorylation, as well as pathway regulation by protein phosphatases [3, 4]. Phosphorylation is of special interest because it provides a rapid and reversible means for the dynamic control of signaling. Thus, the activity of any MAP kinase reflects a balance of the activating kinases and inactivating phosphatases.

Previous computational analysis highlighted the role of MAP kinase phosphatases in determining the timing and duration of MAP kinase activation [5]. That analysis demonstrated that a MAP-kinase-induced increase in phosphatase expression moves the signaling network from a bistable state, in which a brief stimulus results in sustained MAP kinase activation, to a monostable state in which the system responds in a manner proportional to the stimulus. In yeast, phosphatases have likewise been proposed to play a critical role in MAP kinase signaling. For example, activation of the MAP kinase Hog1 leads to enhanced expression of protein Tyr-phosphatases Ptp2 and Ptp3, but the induction in this case is rather modest and occurs too slowly to explain the rapid inactivation of Hog1 [6, 7].

To better understand the dynamics of signal regulation, we investigated the high-osmolarity glycerol response pathway mediated by Hog1 in yeast [8]. Hog1 is required for cell adaptation to osmotic-stress conditions [9] and does so through increased production of a compatible solute that serves to equalize cellular osmotic pressure with the external environment. The nature of the solute differs in various organisms, but in yeast it is glycerol. Yeast mutants that cannot produce or retain glycerol show diminished viability after an osmotic shock despite strongly enhanced Hog1 phosphorylation. On the other hand constitutive, or nontransient, activation of Hog1 leads to cell death. Therefore, strict control over the dynamics of Hog1 activation is essential for cell survival [8].

High osmolarity stimulates at least two putative osmosensing proteins, Sho1 and Sln1, that independently activate Hog1. Sln1 is an integral membrane protein homologous to bacterial two-component signal transducers. Upon stress stimulation, Sln1 activates two partially redundant kinases (Ssk2 and Ssk22), which then activate the MAP kinase kinase Pbs2 and ultimately Hog1. The second osmosensor Sho1 binds and activates a distinct MAP kinase kinase kinase Ste11, which then activates Pbs2 and Hog1. Although they are widely referred to as osmosensing "receptors," Sho1 and Sln1 are not likely to serve as receptors in the usual sense because they respond to such a wide range of chemically distinct substances. Indeed the transmembrane domains of Sho1 are not specifically required to sense changes in osmolarity or even to activate the Hog1

*Correspondence: hdohlman@med.unc.edu

pathway [10]. Rather, these osmosensing proteins may be activated through a physical stimulus that accompanies cell shrinkage or membrane remodeling.

The utility of multiple branches converging on a single MAP kinase is not established, but it may help the cell to respond over a wide range of osmolarity changes [11]. Whereas the Sln1 branch responds in a linear fashion up to approximately 600 mM NaCl, Sho1 operates in an all-or-none fashion. The Sho1 branch is considered here because activation of Hog1 is in this case unusually transient, whereas activation by Sln1 is more persistent. Moreover, the all-or-none behavior of the Sho1 branch is highly characteristic of a system that is subject to feedback regulation.

We began our analysis by first developing simple mathematical models of Hog1 signaling and its regulation. These models predicted the existence of a key regulatory event, occurring early in the pathway, that requires Hog1 kinase activity. Our experimental analysis revealed that Hog1 phosphorylates Sho1. Moreover, we found that Sho1 exists normally as a homo-oligomer and that phosphorylation leads to loss of Sho1 oligomerization and diminished signaling. These events constitute a novel negative-feedback loop contributing to the control of Hog1 activation. Further computational analysis indicates that multicomponent signaling cascades allow cells to respond to a wide range of signal inputs, in addition to providing an effective means of signal amplification. Given the conservation of MAP kinase signaling in all eukaryotes, the mechanisms outlined here are likely to be applicable to other signaling pathways in yeast as well as in animals.

Results

Computational Modeling

Our goal here was to identify new mechanisms of regulation, focusing specifically on the osmotic-stress-response pathway mediated by Hog1. Initially, we compared Hog1 activation by either the Sln1 branch alone (in a *sho1*Δ mutant) or the Sho1 branch alone (in an *ssk1*Δ mutant). Cells were exposed to high concentrations of KCl (hereafter "salt"), and the corresponding cell lysates were resolved by immunoblotting. These blots were then probed with phospho-p38 antibodies, which recognize the dually phosphorylated and activated form of Hog1. In this comparison, we found that signaling from the Sho1 branch is more transient than the Sln1 branch (Figure 1A), as reported previously [8]. Because our interest was in mechanisms of short-term adaptation, we restricted our investigations to the Sho1 branch of the pathway.

To better guide our analysis, we began by constructing a series of simple mathematical models of Hog1 activity. This approach requires quantitative information about the dose dependence and duration of pathway activation. Accordingly, Figure 1B shows a measured time series for Hog1 phosphorylation in the presence of different concentrations of salt. In this analysis, phospho-Hog1 increased rapidly, peaking at approximately 5 min, and was followed by a decrease to basal levels within 30 min. This behavior was strongly dose dependent in light of the fact that 2-fold changes in salt concentration resulted in dramatic differences in phospho-Hog1 levels. Moreover, Hog1 appears to regulate its own activity because a catalytically inactive mutant (described below) reached a much higher level of maximum phosphorylation and failed to return to baseline levels even after 60 min of stimulation (Figure 1C) [6].

We then used the available data to construct mathematical models of Hog1 inactivation. Given the striking differences between Hog1 phosphorylation in the absence and presence of kinase activity, all of our models invoked some Hog1-dependent phosphorylation event. We did not consider other known mechanisms of adaptation such as alterations in glycerol synthesis or export, either because they occur too slowly or do not appear to be regulated by Hog1. Each model was then evaluated for its ability to reproduce our experimental data and for consistency with previously published experimental observations [12]. The first model invokes Hog1-mediated activation of a downstream negative regulator (Figure 1E, model I). The model does not dictate a specific substrate, but we considered a protein phosphatase as the likely target. Phosphorylation of both Thr-174 and Tyr-176 within the activation loop of Hog1 is necessary for its activation, so dephosphorylation of either residue is sufficient for inactivation. Hog1 is known to be down-regulated by the Tyr-specific phosphatase Ptp2 and to a lesser extent Ptp3 [6, 7]. Thus, we considered Ptp2 as a possible substrate for Hog1 phosphorylation. In this scenario, Hog1 might phosphorylate and activate Ptp2, which could in turn dephosphorylate and inactivate Hog1. The data and model equations that govern this system are provided in the Supplemental Data available online. Mathematical analysis of the model revealed that this mechanism can indeed account for the transient activation of Hog1, as measured by phospho-Hog1 immunoblotting. Figure 1F shows a comparison of simulated (line) and experimentally measured (symbols) time series for phospho-Hog1 abundance at each of three different salt concentrations tested. According to this model, phospho-Hog1 rises rapidly, and this is followed by a gradual increase in phospho-Ptp2 to levels sufficient for deactivating the pathway and restoring phospho-Hog1 to near-basal levels. Moreover, this model requires that phosphorylation increases Ptp2 phosphatase activity by 100-fold. We consider this large effective increase in activity to be plausible given that Ptp2 is predominantly nuclear [13] and only interacts with phospho-Hog1 after the kinase is activated and translocates from the cytoplasm to the nucleus [14, 15]. Note that even when we assume such a large increase in phosphatase activity, however, the model does not completely capture the return to near-basal levels of phospho-Hog1 as observed with 0.5 M salt. Furthermore, deletion of the *PTP2* gene produces only a modest increase in phospho-Hog1 and no change in the temporal behavior of Hog1 phosphorylation (Figure 1D) [6, 7]. In striking contrast, Hog1 phosphorylation was dramatically increased and prolonged when the kinase was mutationally inactivated (Figure 1C). These data suggest that additional mechanisms contribute to pathway deactivation.

Thus, although model I invokes Hog1 activation of a negative regulator, we next considered an alternative model in which Hog1 mediates inactivation of a positive regulator (Figure 1E, model II). As in model I, we assumed

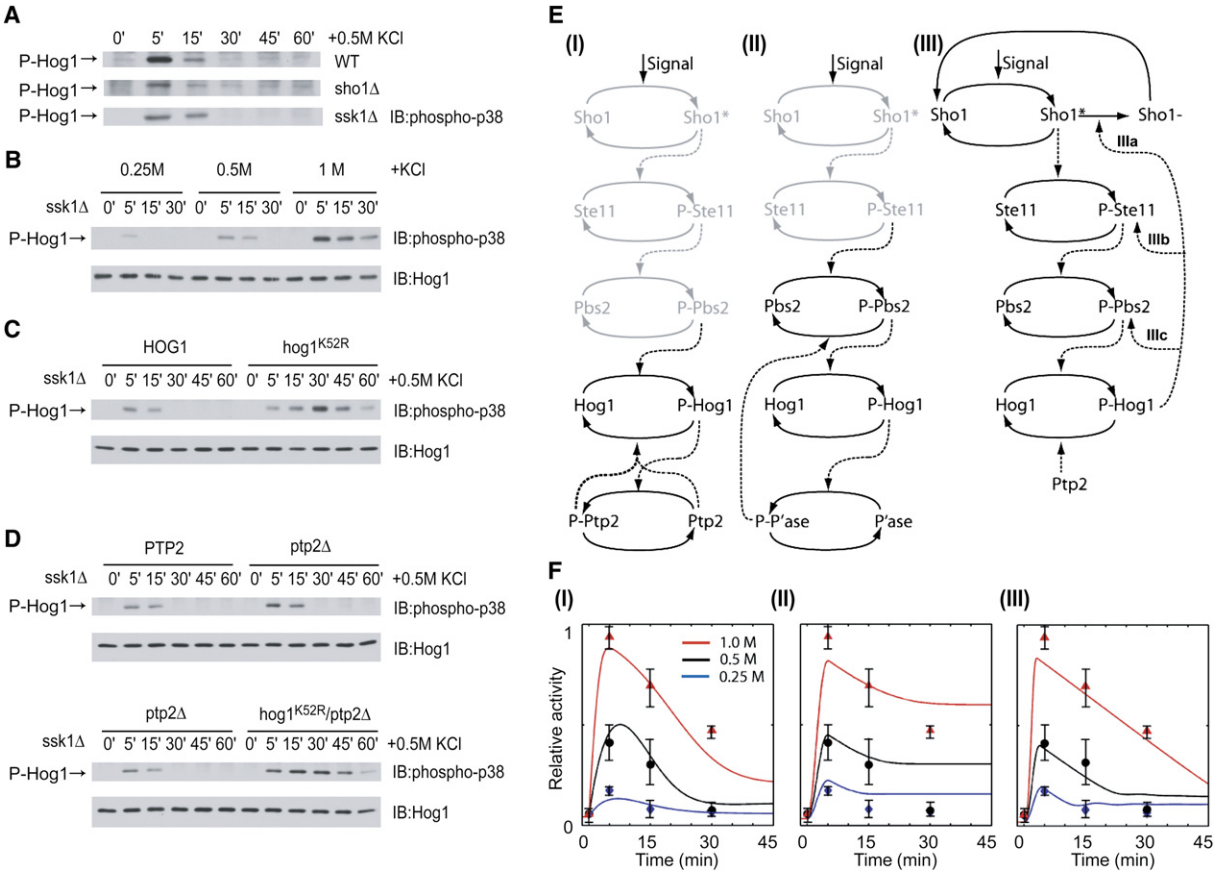

Figure 1. Hog1 Kinase Activity Is Required for Transient Pathway Activation

(A) For determining the kinetics of activation by the Sho1- and Sln1/Ssk1-mediated signaling pathways, *sho1*Δ or *ssk1*Δ mutants, respectively, were treated with 0.5 M KCl for the times indicated; cell lysates were then resolved by 10% SDS-PAGE and immunoblotting (IB) with phospho-p38 antibodies, which recognize the dually phosphorylated and activated form of Hog1.

(B) For determining the dose-response relationship of Sho1 activation, *ssk1*Δ cells were treated with different concentrations of KCl for 15 min and subjected to immunoblotting with anti-phospho-p38 or anti-Hog1 (loading control).

(C) For determining the contribution of Hog1-mediated phosphorylation on its own activity, *ssk1*Δ (HOG1) cells or isogenic cells bearing a catalytically inactive gene replacement mutant (hog1^{K52R}) were treated with KCl and analyzed by immunoblotting.

(D) For determining the contribution of Ptp2-mediated dephosphorylation on Hog1 activation, *ssk1*Δ (PTP2) cells, isogenic *ptp2*Δ mutants, *hog1*^{K52R} mutants, or *ptp2*Δ *hog1*^{K52R} double-mutant cells were treated with KCl and analyzed by immunoblotting.

(E) Three models of Hog1 regulation, as detailed in the text.

(F) Scanning densitometry of data from three or more independent experiments were averaged (from [B], symbols) and plotted together with simulated data for each of the three models presented in ([E], lines). Error bars represent ± SEM.

that phosphorylation by Hog1 activates a phosphatase, but in this case the phosphatase acts on a component early in the pathway such as the MAP kinase kinase Pbs2. To simplify our analysis, we did not explicitly model the step involving Hog1 phosphorylation of the phosphatase. Rather, the rate of dephosphorylation of the upstream kinase was assumed to be proportional to the amount of phospho-Hog1 (see Supplemental Data). This approximation assumes a single rate-limiting step in the negative-feedback loop. That is, either phosphorylation of the phosphatase or dephosphorylation of the intermediate kinase is rate limiting.

Mathematical analysis of this system reveals that it is not capable of generating a phospho-Hog1 response that is transient and that returns to near-basal levels within 30 min of stimulation (Figure 1F, model II, and Supplemental Data). This is because deactivation of Hog1 requires that the intermediate kinase also return to a near baseline level of activity. However, a return to baseline requires that phospho-Hog1 levels remain elevated to counteract the effect of the incoming signal. Given this inherent contradiction, and the model's inability to capture the observed behavior of the system, we eliminated model II from further consideration.

The third mechanism we considered is one in which pathway deactivation occurs through feedback inhibition of an upstream component (Figure 1E, model III). That is, phosphorylation by Hog1 causes a pathway component to enter a state in which it is no longer available for signaling. Moreover, we considered three potential targets for regulation: the osmosensor Sho1 (model IIIa), the MAP kinase kinase kinase Ste11 (includes Ste50, model IIIb), and the MAP kinase kinase Pbs2 (model IIIc) (see Supplemental Data). Modeling all three targets produced a good fit to the time-series data at each of the three salt concentrations tested. Therefore, to further constrain the models and test their validity, we performed additional experiments in which

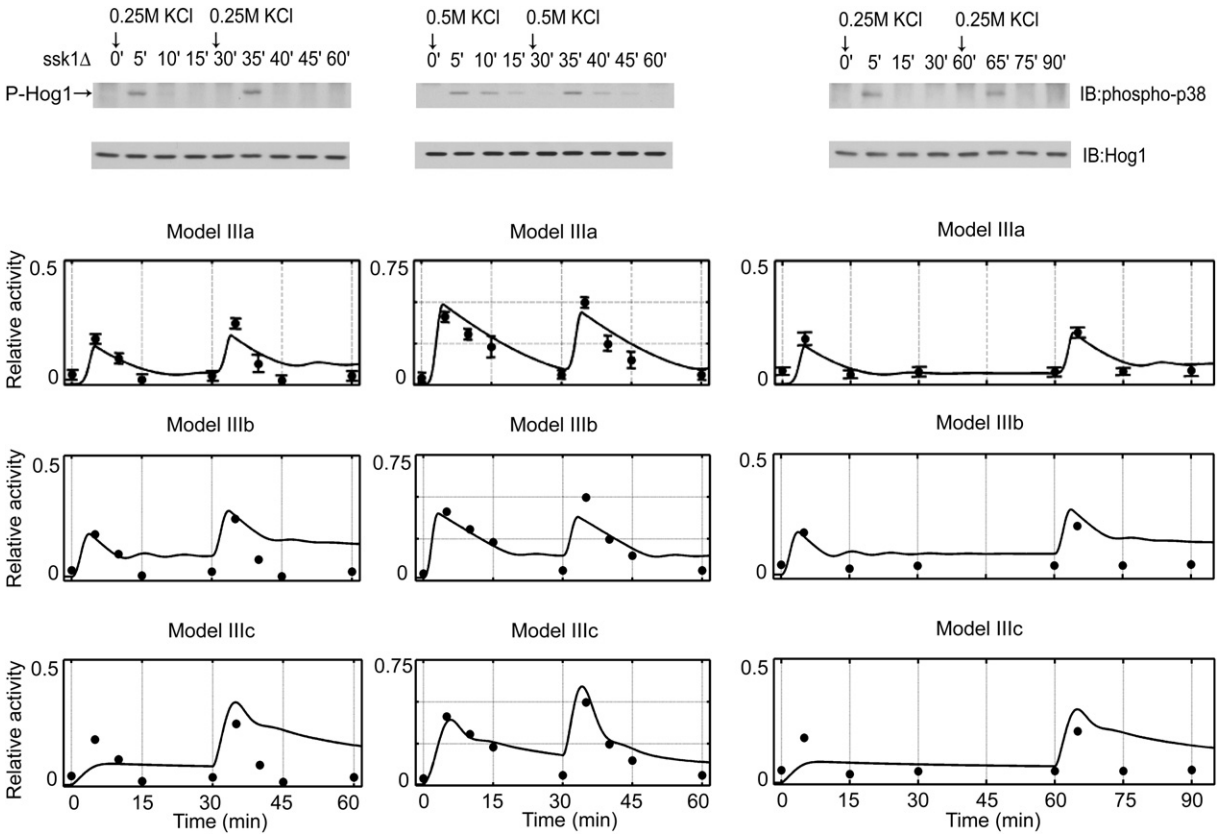

Figure 2. Activation of Hog1 Leads to an Attenuated Response to a Subsequent Stimulus

For refining the computational model, *ssk1*Δ cells were treated twice with the same dose of KCl either 30 min apart or 60 min apart, and cell lysates were then resolved by 10% SDS-PAGE and immunoblotting (IB) with anti-phospho-p38 and anti-Hog1 (top panels). Scanning densitometry of experimental data (symbols) from three or more independent experiments were plotted together with simulated data (lines) from models IIIa, IIIb, and IIIc (bottom panels) as outlined in Figure 1E. Error bars represent ± SEM.

cells were stimulated repeatedly with salt. Cells were treated with either 0.25 M or 0.5 M KCl and then with a second identical treatment after 30 min or 1 hr. As shown in Figure 2, the second dose produced a phospho-Hog1 response that was more transient and only slightly greater than the first, despite a doubling of the final salt concentration (compare Figure 2 and Figure 1B). When we included these new data, only model IIIa (in which Sho1 is the target of feedback inhibition) fully predicted the activity at each time point (Figures 1F and 2). Model IIIc, which invokes regulation of Pbs2, was not sufficiently sensitive at low salt concentrations and also failed to reproduce the amplitude of the second peak of activation (Figure 2). This model also was not capable of capturing the near perfect adaptation (return to baseline activity) observed experimentally. In contrast, regulation of Ste11 or Sho1 introduces additional time delays between Hog1-mediated phosphorylation and diminished Hog1 activation and thereby preserves the ability of cells to respond to low levels of stimulation. However, with Ste11 as the target, the model still produced a significantly worse fit to the data than when Sho1 was the target. These results suggest that a feedback control mechanism, in which the osmosensor Sho1 is phosphorylated and desensitized by Hog1, could best account for the transient behavior of the pathway. This supposition was tested experimentally.

Phosphorylation of Sho1

Model III predicts that Hog1 phosphorylates and desensitizes a component in the pathway upstream of the kinase. Model IIIa invokes Sho1 as the most likely substrate. In order to determine whether Sho1 is indeed phosphorylated, we performed large-scale purification of a functional C-terminally FLAG-tagged version of the protein, expressed in either osmotic-stress-stimulated or unstimulated cells. The purified Sho1-FLAG was subsequently analyzed by SDS-PAGE, in-gel protease digestion, and mass spectrometry. By this approach, Sho1 was unambiguously identified by mass fingerprinting as well as by tandem-mass-spectrometry sequencing (data not shown). In addition, results from tandem-mass-spectrometry analysis of Sho1-specific peptides revealed phosphorylation at Ser-166. This modification was only detected in protein from osmotic-stress-stimulated cells and occurs within a MAP kinase consensus site (Ser or Thr followed by Pro) (data not shown).

To quantitatively monitor phosphorylation, we immunopurified Sho1-FLAG from stress-stimulated and unstimulated cells. Sho1 was then resolved by SDS-PAGE and immunoblotting with a FLAG antibody. As shown in Figure 3, Sho1 normally migrates at ~45 kDa, whereas a second ~47 kDa species accumulates in stimulated cells. Many phosphorylated proteins migrate

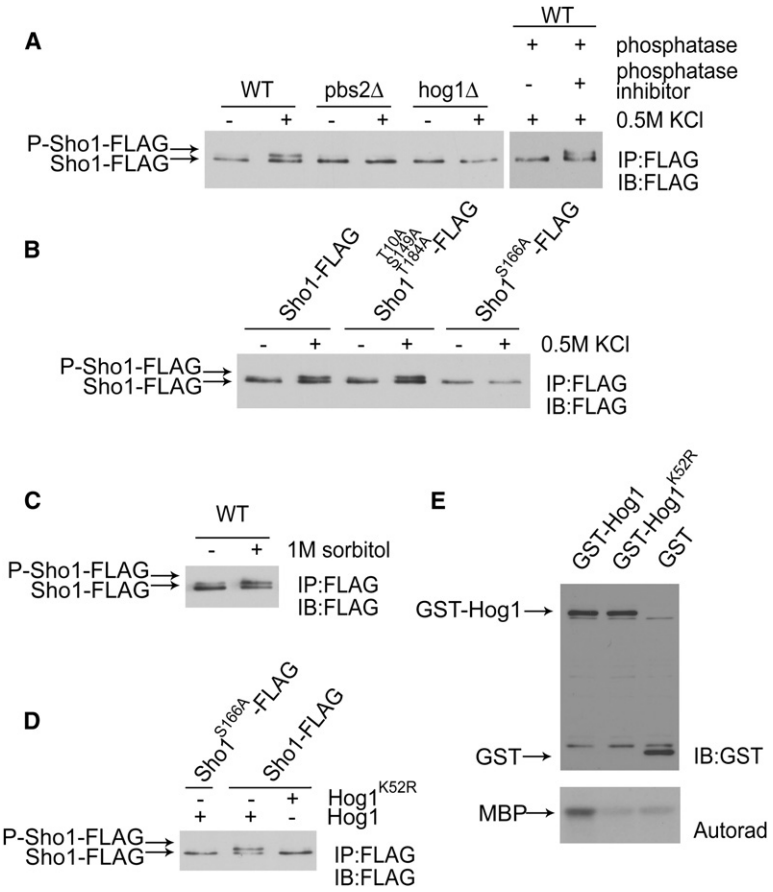

Figure 3. Sho1 Is Phosphorylated by Hog1 at Ser-166

(A) For determining whether Sho1 is phosphorylated, plasmid pRS315 containing a C-terminal FLAG-tagged form of the protein (Sho1-FLAG) was expressed in *sho1*Δ (WT) or isogenic *pbs2*Δ or *hog1*Δ mutant cells and treated with 0.5 M KCl for 15 min, as indicated (+). Sho1-FLAG was immunopurified (IP) and resolved by 10% SDS-PAGE and immunoblotting (IB). For confirming that the slower-migrating form of the protein is phosphorylated, immunopurified Sho1 was treated with λ-protein phosphatase, either in the presence or absence of phosphatase inhibitor.

(B) For confirming that phosphorylation occurs at Ser-166, this residue as well as all other MAP kinase consensus sites (Thr-10, Ser-149, and Thr-184) were replaced with Ala, either alone or in combination. Cultures were treated with KCl for 15 min, immunopurified, and resolved by immunoblotting, as described above.

(C) For confirming that phosphorylation is induced by osmotic stress generally, and not KCl specifically, cultures were treated with 1 M sorbitol in place of 0.5 M KCl.

(D) For determining whether Hog1 phosphorylates Sho1 directly, Sho1-FLAG and Sho1^{S166A}-FLAG (negative control) were immunopurified from a *sho1*Δ *pbs2*Δ mutant strain (to block basal phosphorylation) and mixed with recombinant Hog1 or the catalytically inactive Hog1^{K52R} (negative control) purified from yeast. Sho1 phosphorylation was monitored by immunoblotting as described above. Note that a very faint band comigrating with the phosphorylated form of Sho1 could be detected with longer exposures in all lanes; however, this band is likely to be nonspecific because it was not altered by KCl treatment, by deletion of *HOG1* or *PBS2*, or by Ala substitution of all four MAP kinase consensus sites (data not shown).

(E) For confirming that Hog1^{K52R} lacks catalytic activity, GST-tagged Hog1, Hog1^{K52R}, or GST alone (IB: GST) were purified from yeast treated with 0.4 M NaCl for 10 min. GST fusions were mixed with ^{32}P-γ-ATP and myelin basic protein for 3 hr. Reactions were stopped by the addition of SDS-PAGE sample buffer and boiling. Phosphorylated myelin basic protein was detected by SDS-PAGE and autoradiography (Autorad).

anomalously on SDS-PAGE, so the appearance of a higher-molecular-weight species suggested that a significant proportion of Sho1 was phosphorylated and that phosphorylation is stimulus dependent. To confirm that the mobility shift was due to phosphorylation, we treated immunopurified Sho1 with λ-protein phosphatase prior to immunoblot analysis; under these conditions, the mobility shift was eliminated. The effect of phosphatase treatment was reversed by the simultaneous addition of phosphatase inhibitors. Thus, Sho1 appears to undergo stimulus-dependent phosphorylation in vivo.

To determine whether Hog1 kinase activity is needed for Sho1 phosphorylation, we monitored the phosphorylation-dependent mobility shift in cells lacking known components of the Hog1 signaling pathway. As shown in Figure 3A, Sho1 failed to undergo stress-dependent phosphorylation in cells lacking either Hog1 or Pbs2, which is specifically required for Hog1 activation. Therefore, phosphorylation of Sho1 is contingent on Hog1 function.

To confirm that phosphorylation occurs at Ser-166, we replaced this residue with Ala. As shown in Figure 3B, the Sho1^{S166A} mutant failed to undergo a mobility shift in response to osmotic stress. These data suggest that Ser-166 is the primary site of MAP kinase phosphorylation in vivo. In addition to Ser-166, however, there are three other MAP kinase consensus sites within Sho1. As an additional control, we substituted all three of these other candidate sites (Thr-10, Ser-149, and Thr-184) and showed that the triple Ala mutation does not alter the mobility shift in response to pathway activation (Figure 3B). These data indicate that phosphorylation of Ser-166 fully accounts for the stress-dependent change in Sho1 electrophoretic mobility. To confirm that phosphorylation can be induced by osmotic stress, and not only by KCl, we showed a similar mobility shift in cells treated with 1 M sorbitol (Figure 3C).

To rule out the possibility that Sho1 is phosphorylated by an unknown kinase that is itself activated by Hog1, we monitored phosphorylation of Sho1 by using purified recombinant Hog1 [16]. N-terminally GST-tagged Hog1 was purified from bacteria, and FLAG-tagged Sho1 was purified from yeast. When combined with purified Hog1, Sho1 underwent the same phosphorylation-dependent mobility shift as observed in vivo. In contrast, the Sho1 phosphorylation-site mutant (Sho1^{S166A}) was unchanged after incubation with active Hog1 (Figure 3D). Moreover, phosphorylation required Hog1 kinase activity because the mobility of Sho1 was unaltered by

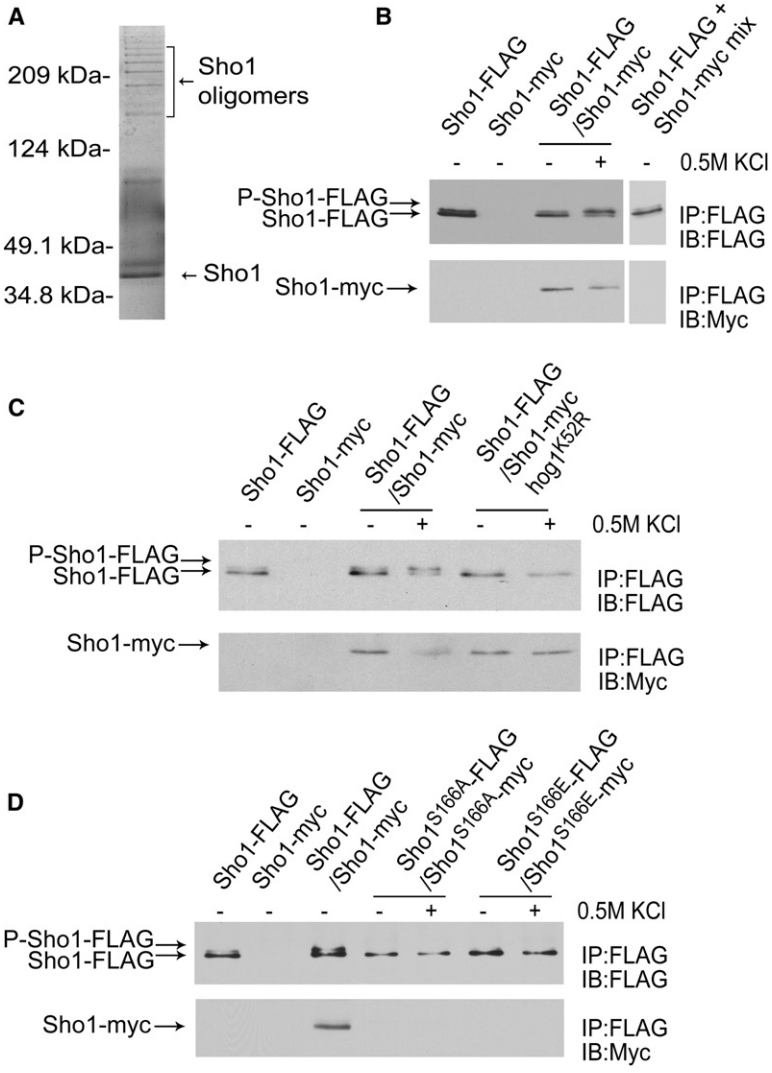

Figure 4. Phosphorylation at Ser-166 Diminishes Sho1 Oligomerization

(A) For obtaining sufficient Sho1 for mass-spectrometry analysis, Sho1-FLAG was immunopurified, resolved by 10% SDS-PAGE, and detected by protein staining. The native species (Sho1) was determined by mass spectrometry to be phosphorylated at Ser-166 (data not shown). The high molecular species (Sho1 oligomers) were shown by mass-spectrometry sequencing to represent Sho1.

(B) For confirming that Sho1 forms a homo-oligomer, *sho1*Δ mutant cells were transformed with plasmid pRS315 containing Sho1-FLAG, pRS316 containing Sho1-Myc, or both (each expressed with the native promoter), detergent-solubilized, immunopurified (IP), and resolved by 10% SDS-PAGE and immunoblotting (IB). For confirming that Sho1 oligomers formed prior to cell disruption, lysates containing Sho1-Myc alone and Sho1-FLAG alone were mixed and then detergent solubilized and immunopurified as described above. Note that Sho1-Myc, like Sho1-FLAG, migrates as a doublet after an osmotic stress (data not shown).

(C) For determining the effect of osmotic stress on Sho1 oligomerization, *sho1*Δ or *sho1*Δ *hog1*^{K52R} mutant cells expressing plasmid-borne Sho1-FLAG, Sho1-Myc, or both were treated with KCl for 15 min and subjected to immunopurification and immunoblot analysis as described above. The relative mobility of the phosphorylated and unphosphorylated bands was demonstrated by resolving these samples in adjacent lanes of the same gel (data not shown).

(D) For determining whether phosphorylation at Ser-166 affects oligomerization of Sho1, the residue was replaced with Cys, Thr (data not shown), Glu (mimics phosphorylated Ser), or Ala. Cells expressing the plasmid-borne wild-type or Sho1 mutants were treated with KCl and subjected to immunopurification and immunoblot analysis as described above.

incubation with a mutant form of the kinase lacking a conserved Lys residue required for catalytic activity (Hog1^{K52R}) (Figures 3D). To confirm that Hog1^{K52R} was catalytically inactive, we purified the protein from yeast and demonstrated that it lacks the ability to phosphorylate a known substrate, myelin basic protein (Figure 3E). Taken together, these results demonstrate unequivocally that Sho1 is phosphorylated by Hog1 directly and that Hog1 phosphorylation occurs at Ser-166.

Homo-Oligomerization of Sho1

In the course of our large-scale purification of Sho1, we detected a ladder of high molecular species by SDS-PAGE (Figure 4A); such laddering is often observed for membrane-bound proteins that exist as oligomers. Indeed, mass spectrometric sequencing of these slower migrating species indicated that they were composed entirely of Sho1.

To establish whether Sho1 normally exists as a homo-oligomeric complex, we immunopurified the protein and tested for coassociation with additional Sho1. To distinguish the purified and copurifying forms of the protein, we coexpressed FLAG- and Myc-tagged Sho1 (both under the control of the native promoter) in a *sho1*Δ mutant. Sho1-FLAG was then purified with an anti-FLAG affinity resin, and any coprecipitating Sho1-Myc was detected with a Myc antibody. By this approach, Sho1-Myc specifically associated with purified Sho1-FLAG (Figure 4B); conversely, Sho1-FLAG specifically associated with purified Sho1-Myc (data not shown). In contrast, no complex was detected if Sho1-Myc and Sho1-FLAG were combined after cell lysis, thereby excluding the possibility that oligomers formed during the course of purification (Figure 4B).

As noted above, Sho1 is phosphorylated and also exists as an oligomer. Thus, we considered whether Sho1 oligomerization might be regulated in a stimulus- or phosphorylation-dependent manner. As shown in Figures 4B and 4C, Sho1 oligomerization was diminished after an osmotic stimulus. In contrast, Sho1 oligomerization was unaffected in cells that express the catalytically inactive Hog1^{K52R} mutant, which cannot phosphorylate Sho1 (Figure 4C). Moreover, whereas immunopurified Sho1-FLAG migrated as a doublet (representing the phosphorylated and unphosphorylated species), the copurifying pool of Sho1-Myc comprised a single band

that comigrates with the unphosphorylated species (Figures 4B and 4C; data not shown). Collectively, these results suggest that the unphosphorylated form of Sho1 is what assembles into an oligomeric complex and that phosphorylation diminishes Sho1 oligomer formation.

We then investigated whether phosphorylation of Ser-166 specifically was responsible for the loss of Sho1 oligomerization. To this end, we coexpressed mutants of Sho1-FLAG and Sho1-Myc in which the phosphorylation-site Ser was replaced with Glu (Sho1^{S166E}). Substitution with a negatively charged amino acid will in many cases mimic the activity of the phosphorylated residue. In this instance, the Sho1^{S166E} mutant failed to form a stable complex when purified with either the FLAG affinity resin (Figure 4D) or the Myc affinity resin (data not shown). Notably, substitution of Ser to Ala, Ser to Cys, or Ser to Thr also inhibited oligomer formation (Figure 4D and data not shown). The simplest explanation for this finding is that Ser-166 constitutes part of the Sho1-Sho1 binding interface, and any alteration of this site diminishes protein-protein interaction. In any case, these data indicate that Sho1 oligomerization is impaired when Ser-166 is modified, either through phosphorylation or mutagenesis.

Functional Characterization of Sho1 Oligomerization

Finally, we investigated how changes in Sho1 oligomerization and phosphorylation affect the osmotic-stress response in vivo. Mutant *sho1*Δ cells were transformed with plasmids expressing wild-type Sho1, the oligomerization-deficient Sho1^{S166A} mutant, the oligomerization-deficient and phospho-mimic Sho1^{S166E} mutant, or no protein. Cells were grown in liquid medium, serially diluted, and spotted onto standard growth medium containing maximally effective doses of salt (see Figure 1B). As shown in Figure 5, cells expressing wild-type Sho1 or Sho1^{S166A} grew substantially better than those expressing Sho1^{S166E}. No difference in growth was observed in standard (low-salt) growth conditions. Furthermore, there was an excellent correlation between cell growth and Hog1 activation. Cells expressing Sho1 or Sho1^{S166A} exhibited a robust Hog1 phosphorylation response, whereas Sho1^{S166E} yielded a substantially diminished response. Given that Ser-166 is evidently required for Sho1 oligomerization, we postulate that salt promotes Sho1 dissociation, and this dissociation serves to unmask the site of phosphorylation. Phosphorylated Sho1 is less able to transmit the signal, and these cells are therefore less able to adapt to osmotic-stress conditions.

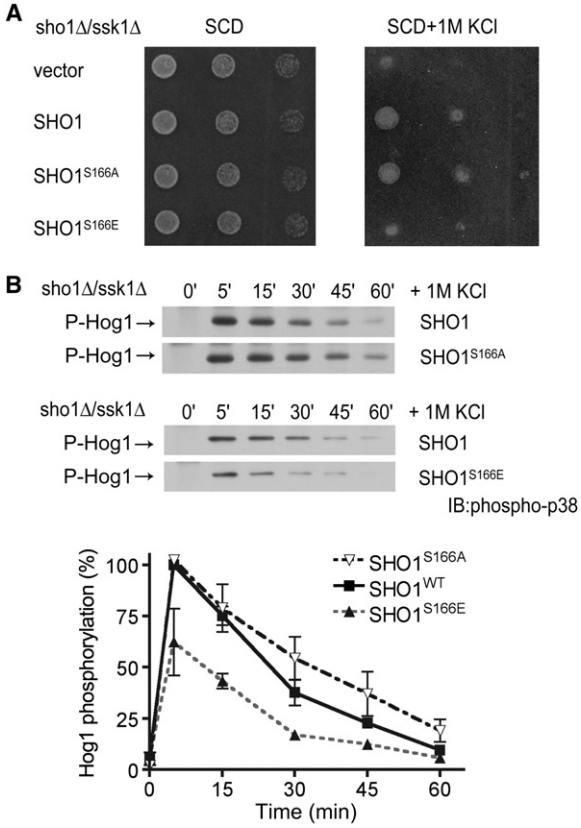

Figure 5. Sho1 Phosphorylation Leads to Diminished Growth Adaptation

(A) For determining how Sho1 phosphorylation affects cellular growth under osmostic stress conditions, *sho1*Δ *ssk1*Δ mutant cells were transformed with plasmid pRS315 containing no insert (vector), Sho1, Sho1^{S166A}, or Sho1^{S166E} and then grown to saturation in liquid medium, serially diluted, and spotted onto solid medium containing 1 M KCl. This dose of KCl confers maximum Hog1 phosphorylation, as shown in Figure 1B. No growth differences were observed at lower doses of KCl (0.5 M) (data not shown). Cell growth was recorded after 3–5 days.

(B) Pathway activation in the same cells was monitored by immunoblotting (IB) with anti-phospho-p38 and anti-Hog1 (data not shown), as described above. Note that wild-type Sho1 (but not Sho1^{S166A}) will be partially phosphorylated and therefore partially desensitized. Note that the pairs of panels are from the same gel but are positioned so that band intensity at each time point can be best compared. The bottom panel shows that scanning densitometry of data from three or more independent experiments were averaged. Error bars represent ± SEM.

Discussion

A common phenomenon in biology is that cellular responses wane over time despite the presence of a sustained stimulus [17]. Familiar examples include desensitization to light, odors, and chemical stimulants such as caffeine or epinephrine. Generally speaking, cell adaptation entails some form of feedback inhibition, where a downstream effector alters the activity of an upstream transducer. For example, many cell-surface receptors are rapidly phosphorylated and endocytosed after stimulation, and these events limit their ability to transmit the signal. Such phosphorylation-mediated negative-feedback mechanisms do not require new protein synthesis and therefore can act rapidly, sometimes within seconds of pathway activation. Other mechanisms can take hours or even days. For instance in the high osmolarity response pathway, protein phosphatases and enzymes required for glycerol production are induced after prolonged exposure to high concentrations of salt [12]. Increased transcription of a negative regulator can certainly limit pathway activation but would be most likely to occur over the relatively long time scale needed for protein synthesis to occur. Thus, in any given system there can be multiple overlapping feedback-regulation mechanisms, each with distinct temporal characteristics, that collectively modulate cellular responsiveness to a given stimulus.

Much of our previous work has focused on regulation of the pheromone response pathway and the MAP kinase Fus3. Here, we have turned our attention to the high osmolarity signaling pathway and the MAP kinase Hog1. Signaling by the Sho1 branch of the pathway is of particular interest because it exhibits unusually transient activation kinetics. We began with a simple computational model of the Sho1 branch of the pathway. This analysis provided new insights into Hog1-dependent regulation, including a number of predictions that we tested experimentally. We show for the first time that (1) Sho1 is an oligomer; (2) Sho1 is phosphorylated; (3) Sho1 is phosphorylated by Hog1; (4) phosphorylation occurs at Ser-166; (5) phosphorylation occurs within minutes of pathway activation; and (6) phosphorylation leads to diminished oligomerization. Collectively, the available data suggest the following model of Sho1 activation and inactivation: Sho1 exists as an oligomer, which upon osmotic stress activates a kinase cascade culminating with Hog1. Activated Hog1 subsequently phosphorylates Sho1 and promotes a transition from the oligomeric to a monomeric form of the protein. Because Sho1^{S166A} signals normally but fails to oligomerize, the transition from oligomer to monomer does not appear to directly alter Sho1 function. Rather, Sho1 dissociation could serve primarily to unmask the phosphorylation site, and it is this phosphorylated form of Sho1 that is attenuated.

In addition to our mathematical-modeling results, there were several other reasons we considered Sho1 as a likely target for feedback phosphorylation. First, Sho1 is the earliest known component of the pathway and therefore well positioned to regulate signal input [18, 19]. Second, another well-characterized MAP kinase in yeast (Fus3) has been shown to phosphorylate several early activators and regulators, including the RGS protein Sst2 [16], the MAP kinase kinase Ste7 [20, 21], and the kinase scaffold protein Ste5 [22]. Third, the temporal differences in Sln1 versus Sho1 signaling suggest that rapid feedback inhibition occurs through some component that is unique to the Sho1 branch of the pathway. Indeed, Sho1 was postulated previously to be a substrate for Hog1 and that feedback phosphorylation in such a case might dictate pathway specificity or in some way dampen cross talk with the pheromone signaling pathway [23].

Functional analysis of the Hog1^{K52R} mutant provided early evidence for a role of phosphorylation in feedback regulation. Thus, all the computational models were built with an assumption that Hog1 activity is required for pathway inhibition. Functional analysis of the Sho1^{S166A} and Sho1^{S166E} mutants further indicates that feedback phosphorylation restricts Hog1 signaling. Moreover, the effects of Sho1 phosphorylation are evident within minutes of pathway activation. Sho1 phosphorylation does not alter the kinetics of Hog1 activation, however, suggesting that other (as yet unidentified) feedback-phosphorylation events contribute to the observed transient behavior. In support of this concept, Hog1^{K52R} exhibits sustained (but diminished) activation even when Sho1 is mutated so as to be constitutively "desensitized" (Sho1^{S166E}; data not shown).

Our computational analysis also provides new insights into feedback regulation of biological systems generally. Our models indicate that it is far more effective to inhibit an activator than to activate an inhibitor. For example, phosphatases are unsatisfactory targets of feedback regulation—at least with respect to temporal regulation—because the targeted kinase can still be rephosphorylated and reactivated, and a very large increase of phosphatase activity would be needed to noticeably dampen signaling. Moreover, if phosphatase activity is contingent on the MAP kinase, that kinase would have to retain partial activity in order to maintain full phosphatase function.

The ability to deactivate the pathway at the level of the "receptor" has at least two additional advantages for the system. First, if there are components shared among multiple signaling pathways (e.g., Ste11), then deactivation of the receptor allows those components to remain competent for transmitting signals from other receptors. Second, regulation of an early component in a multicomponent signaling cascade will increase the sensitivity of the system by creating a delay between the feedback-phosphorylation event early in the pathway and deactivation of a kinase late in the pathway. Such a delay would allow the cell to adapt to strong signals yet remain sensitive enough to detect weak signals. Thus, although multicomponent signaling cascades are well known to confer signal amplification, we propose that multiple components also allow cells to respond appropriately to a wide range of signal strengths.

Experimental Procedures

Strains and Plasmids

Standard methods for the growth, maintenance, and transformation of yeast and bacteria and for the manipulation of DNA were used throughout. All mutations were constructed with the QuikChange site-directed mutagenesis kit (Stratagene) according to the manufacturer's directions. All plasmid open reading frames constructed in this study were sequenced. The yeast *S. cerevisiae* strains used were BY4741 (*MATa leu2*Δ0 *met15*Δ0 *his3*Δ1 *ura3*Δ0) (Research Genetics) or BY4741-derived deletion mutants lacking *sho1*, *ssk1*, *hog1*, *pbs2*, *ste11*, *msb2*, *sho1/msb2* (*sho1::HIS3*, *msb2::KanMX*), *sho1/ste11*(*sho1::HIS3*, *ste11::KanMX*), *sho1/pbs2* (*sho1::HIS3*, *pbs2::KanMX*), *sho1/ssk1* (*sho1::HIS3*, *ssk1::KanMX*), *sho1/hog1* (*sho1::HIS3*, *hog1::KanMX*), *ssk1/hog1*^{K52R} (*ssk1::KanMX*), and *ssk1/sho1/hog1*^{K52R} (*ssk1::KanMX*, *sho1::HIS3*). Plasmids used for gene disruption (pRS316-sho1::HIS3), gene expression (pRS316-SHO1, pRS315-SHO1-FLAG, pRS306-hog1^{K52R}), and protein purification (pGEX-2T6-GST-HOG1, pRS316-ADH-GST-HOG1, and hog1^{K52R} mutants) are described in detail under Supplemental Data.

Large-Scale Purification from Yeast Cells for Mass-Spectrometry Analysis

Yeast cells were grown in selective SCD medium to $A_{600\ nm} \sim 1.0$. All salt treatments were done by dilution of a 2.5 M stock solution of KCl in growth medium. Note that KCl was used instead of NaCl because sodium replaces potassium in some biomolecules and therefore stimulates detoxification responses unrelated to Hog1 signaling [8]. A total of 10 liters of cells was collected, subjected to glass-bead homogenization, and purified with EZview Red anti-FLAG M2 affinity gel (SL04473, Sigma). In-gel tryptic digestion of Sho1 was conducted as described previously [24], except that the gel was fixed with 10% methanol, 7% acetic acid. This was followed by 16 hr incubation with SYPRO Ruby (Molecular Probes), and the peptides were analyzed on a 4700 MALDI-TOF/TOF mass spectrometer (Applied Biosystems) [24].

TCA-Acid Extraction of Protein for Immunoblot Analysis

Cells in early log phase were collected, disrupted with tricholoracetic-acid precipitation and glass-bead vortex homogenization, and

resolved by 10% SDS-PAGE and immunoblotting with phospho-p38 antibodies at 1:500 (9211L, Cell Signaling Technologies), Hog1 (yC-20) antibodies at 1:100 (sc-6815, Santa Cruz Biotechnology), Myc antibodies at 1:1000 (9E10 monoclonal cell culture supernatant), or FLAG antibodies at 1:1000 (F-3165, Sigma). Immunoreactive bands were detected with horseradish peroxidase-conjugated goat anti-mouse IgG or anti-rabbit IgG (Bio-Rad) in conjunction with enhanced chemiluminescence (Amersham Biosciences) according to the manufacturer's instructions. Band intensity was quantified by scanning densitometry with UN-SCAN-IT gel Automated Digitizing System (Silk Scientific Corporation, version 5.1). In each case, the data from three to six independent experiments were averaged.

Immunopurification

Yeast cells were grown in selective SCD medium to $A_{600\ nm} \sim 1.0$ and then collected into ice-cold tubes containing NaN_3 (5 mM final) and centrifuged at 500 × g for 5 min. Cell pellets were immediately frozen and stored at −80°C. Immunopurification was conducted as described previously except 50 mM $NaPO_4$ was used in place of HEPES-NaOH buffer [24]. For phosphatase treatment, the FLAG affinity gel was washed twice with λ-protein phosphatase reaction buffer (50 mM Tris-HCl [pH 7.5], 100 mM NaCl, 2 mM DTT, 0.1 mM EGTA, and 0.01% Brij 35) and incubated with 50 μl λ-protein phosphatase reaction buffer with 0.5 μl λ-protein phosphatase (P0753S, New England Biolabs), with or without phosphatase inhibitors (10 mM Na_3VO_4 and 50 mM NaF) at 30°C for 30 min. After phosphatase treatment, the gel was centrifuged at 500 × g for 30 s and washed once with IP lysis buffer. Protein was eluted with 3× FLAG peptide and resolved by SDS-PAGE and immunoblotting as described above.

Purification of GST-MAP Kinases and In Vitro Phosphorylation Assays

GST-Hog1 and Hog1^{K52R} were purified from *E. coli* as described previously for Fus3 [16]. Hog1 was preactivated for 45 min at 30°C with ATP in kinase buffer, as described previously [16]. Sho1-FLAG substrate was immunopurified from yeast and phosphorylated in vitro with bacterially expressed GST-Hog1 or GST-Hog1^{K52R} as described previously for phosphorylation of Sst2-His6 by GST-Fus3 [16]. Myelin basic protein (Sigma) was phosphorylated in an in vitro kinase reaction with GST-MAP kinases purified from midlog phase yeast treated with 0.4 M NaCl for 10 min.

Supplemental Data

Supplemental Data include additional Experimental Procedures, four figures, and five tables and are available with this article online at http://www.current-biology.com/cgi/content/full/17/8/659/DC1/.

Acknowledgments

We are grateful to Beverly Errede, Wendell Lim, Yuqi Wang, and Corinne Zeller for advice and reagents. This work was supported by National Institutes of Health grant GM073180 and a predoctoral fellowship from the American Heart Association (to N.H.).

Received: October 6, 2006
Revised: February 20, 2007
Accepted: February 21, 2007
Published online: March 15, 2007

References

1. Johnson, G.L., and Lapadat, R. (2002). Mitogen-activated protein kinase pathways mediated by ERK, JNK, and p38 protein kinases. Science *298*, 1911–1912.
2. Marshall, C.J. (1995). Specificity of receptor tyrosine kinase signaling: Transient versus sustained extracellular signal-regulated kinase activation. Cell *80*, 179–185.
3. Morrison, D.K., and Davis, R.J. (2003). Regulation of MAP kinase signaling modules by scaffold proteins in mammals. Annu. Rev. Cell Dev. Biol. *19*, 91–118.
4. Martin, H., Flandez, M., Nombela, C., and Molina, M. (2005). Protein phosphatases in MAPK signalling: We keep learning from yeast. Mol. Microbiol. *58*, 6–16.
5. Bhalla, U.S., Ram, P.T., and Iyengar, R. (2002). MAP kinase phosphatase as a locus of flexibility in a mitogen-activated protein kinase signaling network. Science *297*, 1018–1023.
6. Wurgler-Murphy, S.M., Maeda, T., Witten, E.A., and Saito, H. (1997). Regulation of the Saccharomyces cerevisiae HOG1 mitogen-activated protein kinase by the PTP2 and PTP3 protein tyrosine phosphatases. Mol. Cell. Biol. *17*, 1289–1297.
7. Jacoby, T., Flanagan, H., Faykin, A., Seto, A.G., Mattison, C., and Ota, I. (1997). Two protein-tyrosine phosphatases inactivate the osmotic stress response pathway in yeast by targeting the mitogen-activated protein kinase, Hog1. J. Biol. Chem. *272*, 17749–17755.
8. Hohmann, S. (2002). Osmotic stress signaling and osmoadaptation in yeasts. Microbiol. Mol. Biol. Rev. *66*, 300–372.
9. Brewster, J.L., de Valoir, T., Dwyer, N.D., Winter, E., and Gustin, M.C. (1993). An osmosensing signal transduction pathway in yeast. Science *259*, 1760–1763.
10. Raitt, D.C., Posas, F., and Saito, H. (2000). Yeast cdc42 GTPase and ste20 PAK-like kinase regulate Sho1-dependent activation of the hog1 MAPK pathway. EMBO J. *19*, 4623–4631.
11. Maeda, T., Takekawa, M., and Saito, H. (1995). Activation of yeast PBS2 MAPKK by MAPKKKs or by binding of an SH3-containing osmosensor. Science *269*, 554–558.
12. Klipp, E., Nordlander, B., Kruger, R., Gennemark, P., and Hohmann, S. (2005). Integrative model of the response of yeast to osmotic shock. Nat. Biotechnol. *23*, 975–982.
13. Mattison, C.P., Spencer, S.S., Kresge, K.A., Lee, J., and Ota, I.M. (1999). Differential regulation of the cell wall integrity mitogen-activated protein kinase pathway in budding yeast by the protein tyrosine phosphatases Ptp2 and Ptp3. Mol. Cell. Biol. *19*, 7651–7660.
14. Ferrigno, P., Posas, F., Koepp, D., Saito, H., and Silver, P.A. (1998). Regulated nucleo/cytoplasmic exchange of HOG1 MAPK requires the importin beta homologs NMD5 and XPO1. EMBO J. *17*, 5606–5614.
15. Mattison, C.P., and Ota, I.M. (2000). Two protein tyrosine phosphatases, Ptp2 and Ptp3, modulate the subcellular localization of the Hog1 MAP kinase in yeast. Genes Dev. *14*, 1229–1235.
16. Parnell, S.C., Marotti, L.A., Jr., Kiang, L., Torres, M.P., Borchers, C.H., and Dohlman, H.G. (2005). Phosphorylation of the RGS protein Sst2 by the MAP kinase Fus3 and use of Sst2 as a model to analyze determinants of substrate sequence specificity. Biochemistry *44*, 8159–8166.
17. Dohlman, H.G. (2002). Diminishing returns. Nature *418*, 591.
18. Reiser, V., Salah, S.M., and Ammerer, G. (2000). Polarized localization of yeast Pbs2 depends on osmostress, the membrane protein Sho1 and Cdc42. Nat. Cell Biol. *2*, 620–627.
19. Posas, F., and Saito, H. (1997). Osmotic activation of the HOG MAPK pathway via Ste11p MAPKKK: Scaffold role of Pbs2p MAPKK. Science *276*, 1702–1705.
20. Zhou, Z., Gartner, A., Cade, R., Ammerer, G., and Errede, B. (1993). Pheromone-induced signal transduction in Saccharomyces cerevisiae requires the sequential function of three protein kinases. Mol. Cell. Biol. *13*, 2069–2080.
21. Maleri, S., Ge, Q., Hackett, E.A., Wang, Y., Dohlman, H.G., and Errede, B. (2004). Persistent activation by constitutive Ste7 promotes Kss1-mediated invasive growth but fails to support Fus3-dependent mating in yeast. Mol. Cell. Biol. *24*, 9221–9238.
22. Flotho, A., Simpson, D.M., Qi, M., and Elion, E.A. (2004). Localized feedback phosphorylation of Ste5p scaffold by associated MAPK cascade. J. Biol. Chem. *279*, 47391–47401.
23. O'Rourke, S.M., and Herskowitz, I. (1998). The Hog1 MAPK prevents cross talk between the HOG and pheromone response MAPK pathways in Saccharomyces cerevisiae. Genes Dev. *12*, 2874–2886.
24. Hall, M.C., Torres, M.P., Schroeder, G.K., and Borchers, C.H. (2003). Mnd2 and Swm1 are core subunits of the Saccharomyces cerevisiae anaphase-promoting complex. J. Biol. Chem. *278*, 16698–16705.